

RESEARCH

Open Access



# Molecular identification and functional characterization of a transcription factor GeRAV1 from *Gelsemium elegans*

Tianzhen Cui<sup>1</sup>, Shoujian Zang<sup>1</sup>, Xinlu Sun<sup>1</sup>, Jing Zhang<sup>1</sup>, Yachun Su<sup>1</sup>, Dongjiao Wang<sup>1</sup>, Guran Wu<sup>1</sup>, Ruiqi Chen<sup>2</sup>, Youxiong Que<sup>1</sup>, Qing Lin<sup>2,3\*</sup> and Chuihuai You<sup>1,2,3\*</sup>

## Abstract

**Background** *Gelsemium elegans* is a traditional Chinese medicinal plant and temperature is one of the key factors affecting its growth. RAV (related to ABI3/VP1) transcription factor plays multiple roles in higher plants, including the regulation of plant growth, development, and stress response. However, RAV transcription factor in *G. elegans* has not been reported.

**Results** In this study, three novel *GeRAV* genes (*GeRAV1-GeRAV3*) were identified from the transcriptome of *G. elegans* under low temperature stress. Phylogenetic analysis showed that *GeRAV1-GeRAV3* proteins were clustered into groups II, IV, and V, respectively. RNA-sequencing (RNA-seq) and real-time quantitative PCR (qRT-PCR) analyses indicated that the expression of *GeRAV1* and *GeRAV2* was increased in response to cold stress. Furthermore, the *GeRAV1* gene was successfully cloned from *G. elegans* leaf. It encoded a hydrophilic, unstable, and non-secretory protein that contained both AP2 and B3 domains. The amino acid sequence of *GeRAV1* protein shared a high similarity of 81.97% with *Camptotheca acuminata* CaRAV. Subcellular localization and transcriptional self-activation experiments demonstrated that *GeRAV1* was a nucleoprotein without self-activating activity. The *GeRAV1* gene was constitutively expressed in the leaves, stems, and roots of the *G. elegans*, with the highest expression levels in roots. In addition, the expression of the *GeRAV1* gene was rapidly up-regulated under abscisic acid (ABA), salicylic acid (SA), and methyl jasmonate (MeJA) stresses, suggesting that it may be involved in hormonal signaling pathways. Moreover, *GeRAV1* conferred improved cold and sodium chloride tolerance in *Escherichia coli* Rosetta cells.

**Conclusions** These findings provided a foundation for further understanding on the function and regulatory mechanism of the *GeRAV1* gene in response to low-temperature stress in *G. elegans*.

**Keywords** *Gelsemium elegans*, RAV transcription factor, Cold tolerance, Expression analysis, Prokaryotic expression

\*Correspondence:

Qing Lin  
miranda100816@126.com  
Chuihuai You  
you123chui@163.com

<sup>1</sup>Key Laboratory of Sugarcane Biology and Genetic Breeding, Ministry of Agriculture and Rural Affairs, Key Laboratory of Genetics, Breeding and

Multiple Utilization of Crops, Ministry of Education, College of Agriculture, Fujian Agriculture and Forestry University, Fuzhou 350002, China

<sup>2</sup>College of Life Sciences, Fujian Agriculture and Forestry University, Fuzhou 350002, China

<sup>3</sup>The Second People's Hospital, Fujian University of Traditional Chinese Medicine, Fuzhou, Fujian 350003, China



© The Author(s) 2023. **Open Access** This article is licensed under a Creative Commons Attribution 4.0 International License, which permits use, sharing, adaptation, distribution and reproduction in any medium or format, as long as you give appropriate credit to the original author(s) and the source, provide a link to the Creative Commons licence, and indicate if changes were made. The images or other third party material in this article are included in the article's Creative Commons licence, unless indicated otherwise in a credit line to the material. If material is not included in the article's Creative Commons licence and your intended use is not permitted by statutory regulation or exceeds the permitted use, you will need to obtain permission directly from the copyright holder. To view a copy of this licence, visit <http://creativecommons.org/licenses/by/4.0/>. The Creative Commons Public Domain Dedication waiver (<http://creativecommons.org/publicdomain/zero/1.0/>) applies to the data made available in this article, unless otherwise stated in a credit line to the data.

## Background

Under low temperature stress, plants undergo significant alterations in morphology, physiology, molecular biology, and metabolism, leading to functional disruption and impairments in growth and development [1]. Transcription factors (TFs) are the major regulators in response to and coping with cold stress in plants [2]. The primary signal transduction pathways were activated in plants under low temperature stress depend on inducer of C-repeat binding factor expression/dehydration response elements binding protein (ICE-CBF/DREB) [3]. Besides, TFs like WRKY, leucine zipper (bZIP), v-myb avian myeloblastosis viral oncogene homolog (MYB), and NAC (NAM, ATAF1/2, CUC2) are capable of regulating gene expression and activating cold-regulated genes (CORs) [3]. The APETALA2/ethylene-responsive factor (AP2/ERF) family, which can be categorized into subfamilies including AP2, ERF, RAV, and Soloist, is one of the most extensive groups of TFs in plants [4]. Among them, RAV TFs, which not only contain AP2 domains but also have a B3 domain, are the specific class of TFs in higher plants, and are also classified as a B3 superfamily. The AP2 domain consisting of about 60 amino acids, which can recognize the CAACA motif, is located at the N-terminus of the RAV protein [4, 5]. Conversely, the B3 domain consisting of about 110 amino acids, which can recognize the CACCTG motif, is located in the conserved region at the C-terminus of the RAV protein [6]. Interesting, the presence of both domains in RAV TFs can enhance the specificity and affinity of binding to targeted DNA for controlling gene expression [4, 5].

Not surprisingly, in the AP2/ERF family, RAV TFs containing both AP2 and B3 domains have received increasing attention. In 1999, two novel RAV TFs (RAV1 and RAV2) have been identified for the first time from *Arabidopsis thaliana* [5]. Subsequent study has proved that there are 13 RAV TFs in *A. thaliana*, six of which contain both AP2 and B3 domains, including AtRAV1 (At1g13260), AtTEM1 (At1g25560), AtTEM2 (At1g68840), At3g25730, At1g50680, and At1g51120 [6]. The RAV family genes involved in plant growth and development and response to various stresses have been successively reported [7]. Overexpression of *Zea mays* *ZmRAV1* can enhance salt and osmotic tolerance in transgenic *A. thaliana* [8]. The promoter region of the RAV subfamily contains cis-acting elements involving low temperature response (LTR), and can thus regulate gene expression under cold stress [9]. Early cold stress rapidly induces overexpression of the *BcRAV* gene in *Brassica campestris* and improves its cold resistance [10]. The *VaRAV1* gene in *Vitis amurensis* plays a significant role in cold stress by regulating related TFs and inducing the expression of related genes in the cell wall [11]. To sum up, one hand, RAV TFs can regulate plant

seed development, root growth, flower opening, and leaf senescence [12–15]. On the other hand, RAV TFs play important roles in biotic and abiotic stresses in plants, including disease, cold, drought, and salt resistance [8, 10, 16].

*Gelsemium elegans* (Gardner and Champ.) Benth., the medicinal vine plant commonly known as Gelsemium or “heartbroken grass”, was first recorded in the traditional Chinese medicinal book “Shennong Materia Medica”. Although the entire plant of *G. elegans* is highly toxic, it has a high medicinal value [17]. The effective active components of *G. elegans* were indole alkaloids. Over a hundred different types of monoterpene indole alkaloids have been extracted from the roots [18], stems, leaves [19], fruits [20], and other organs of *G. elegans*, which provide a valuable reference for the development of new drugs [21, 22]. Researches have shown that the alkaloids in *G. elegans* are pharmacologically active in pain relief [23], anti-inflammatory effects [24], immunomodulatory [25], and therapeutic for depression and anxiety [26]. Surprisingly, nearly half of the common drugs come from natural products, especially alkaloids, making alkaloid-rich medicinal plants the center of attention [27]. *G. elegans* mainly grows in Southeast Asia and southern China [28]. Low temperature can affect the growth, metabolite biosynthesis and gene expression of medicinal plants, such as *Angelica sinensis* [29], *Dysosma versipellis* (Hance) M. Chang [30], and *Podophyllum hexandrum* Royle [31]. Similarly, *G. elegans* cannot tolerate low temperatures during its growth. Prolonged exposure to low temperatures leads to morphological and physiological changes in *G. elegans*, which may affect the content and activity of its active ingredients [32].

Currently, there is still no report on the role of RAV TFs from *G. elegans* in cold tolerance. In this study, three RAV subfamily genes were identified and analyzed from the *G. elegans* transcriptome database constructed by our research group under low temperature stress (unpublished). Based on the transcriptome data and qRT-PCR analysis, one *G. elegans* *GeRAV1* gene significantly induced by 4°C low temperature was successfully cloned. Besides, the sequence characteristics, protein properties, structural domains, phylogenetic tree, subcellular localization, and self-activation activity of the *GeRAV1* gene were analyzed. Its expression in different *G. elegans* tissues and hormone treatments was detected by qRT-PCR technique. Moreover, the tolerance of *GeRAV1* to abiotic stress was investigated using prokaryotic expression systems. The findings of this study should serve as a basis for further exploration of the function and regulatory mechanism of RAV TFs in the response of *G. elegans* to low-temperature stress.

**Results**

**Identification and sequence analysis of *G. elegans* RAV subfamily genes**

Three *GeRAV* genes (*GeRAV1*, c23896.graph\_c0; *GeRAV2*, c34018.graph\_c1; and *GeRAV3*, Gec35851.graph\_c0) were identified from the transcriptome of *G. elegans* under 4°C low temperature stress which was previously constructed by our research group. According to those reports on the whole-genome analysis of the RAV gene family [33–35], a phylogenetic tree was constructed using the protein sequences of the *GeRAV* proteins and RAVs from two dicot plants (*A. thaliana* and *Glycine*

*max*) and three monocot plants (*Z. mays*, *Oryza sativa*, and *Triticum aestivum*) (Fig. 1). A total of 77 RAV proteins were divided into five groups (Group I–V). Interestingly, *GeRAV1* was clustered into Group II with proteins containing AP2 and B3 domains, and the other two *GeRAVs* (*GeRAV2* and *GeRAV3*) were clustered into two respective groups (Group IV and Group V) containing only B3 domains. A total of ten conserved motifs were predicted for RAV proteins using the MEME website and 37.7% of RAV proteins contained more than nine motifs (Fig. 2). From the N-terminus to the C-terminus, all 77 RAV proteins contained motifs 3, 2, and 1, suggesting

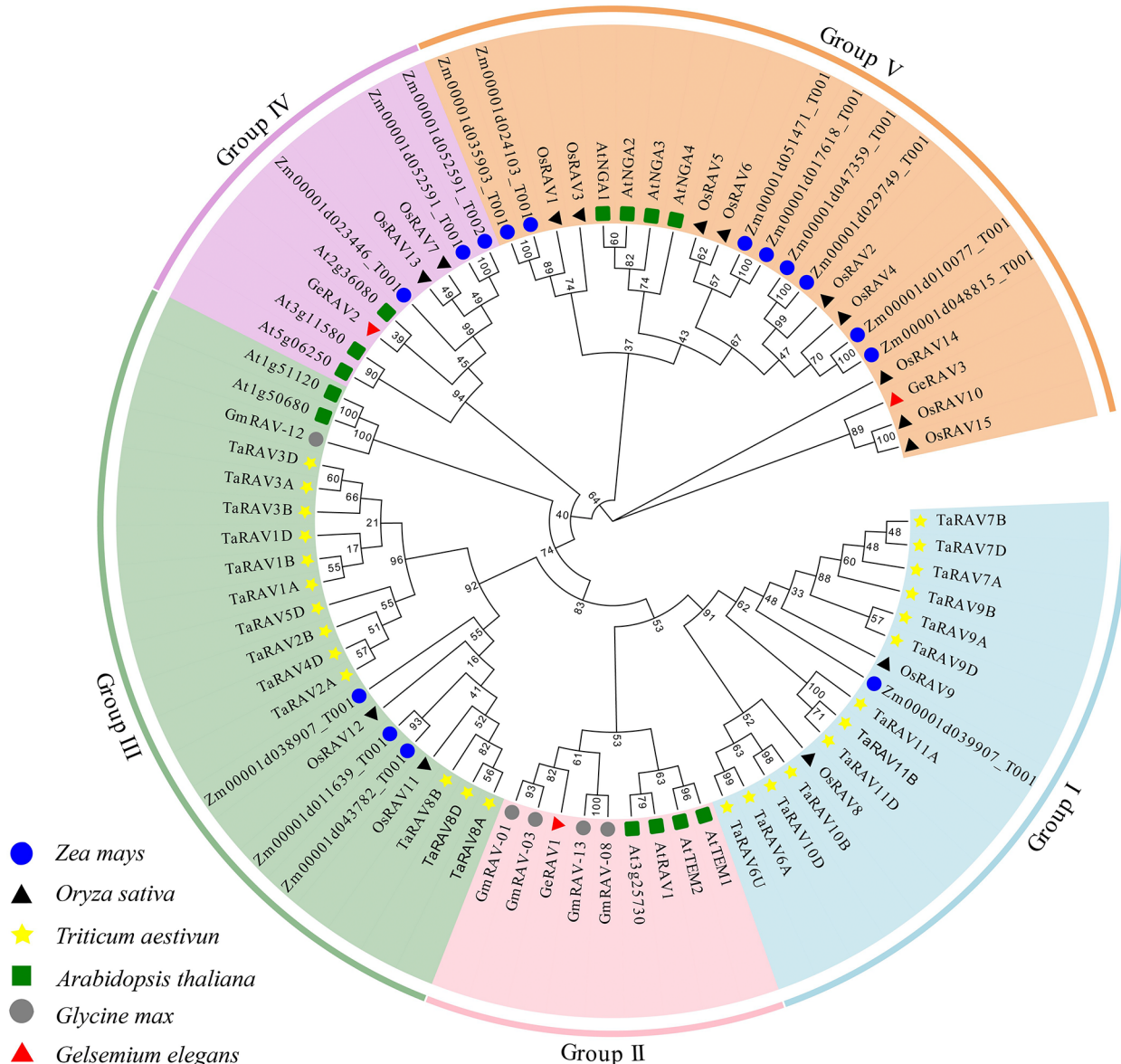


**Fig. 1** Phylogenetic tree of *GeRAVs* and other plant RAV proteins. The RAVs used in the phylogenetic tree analysis were from three dicot species (*Gelsemium elegans*, *Glycine max*, and *Arabidopsis thaliana*) and three monocot species (*Triticum aestivum*, *Oryza sativa*, and *Zea mays*) [33–35]. The GenBank accession numbers of all RAV homologous proteins were listed in Table S5. Groups I–V were marked in blue, pink, green, purple, and orange, respectively

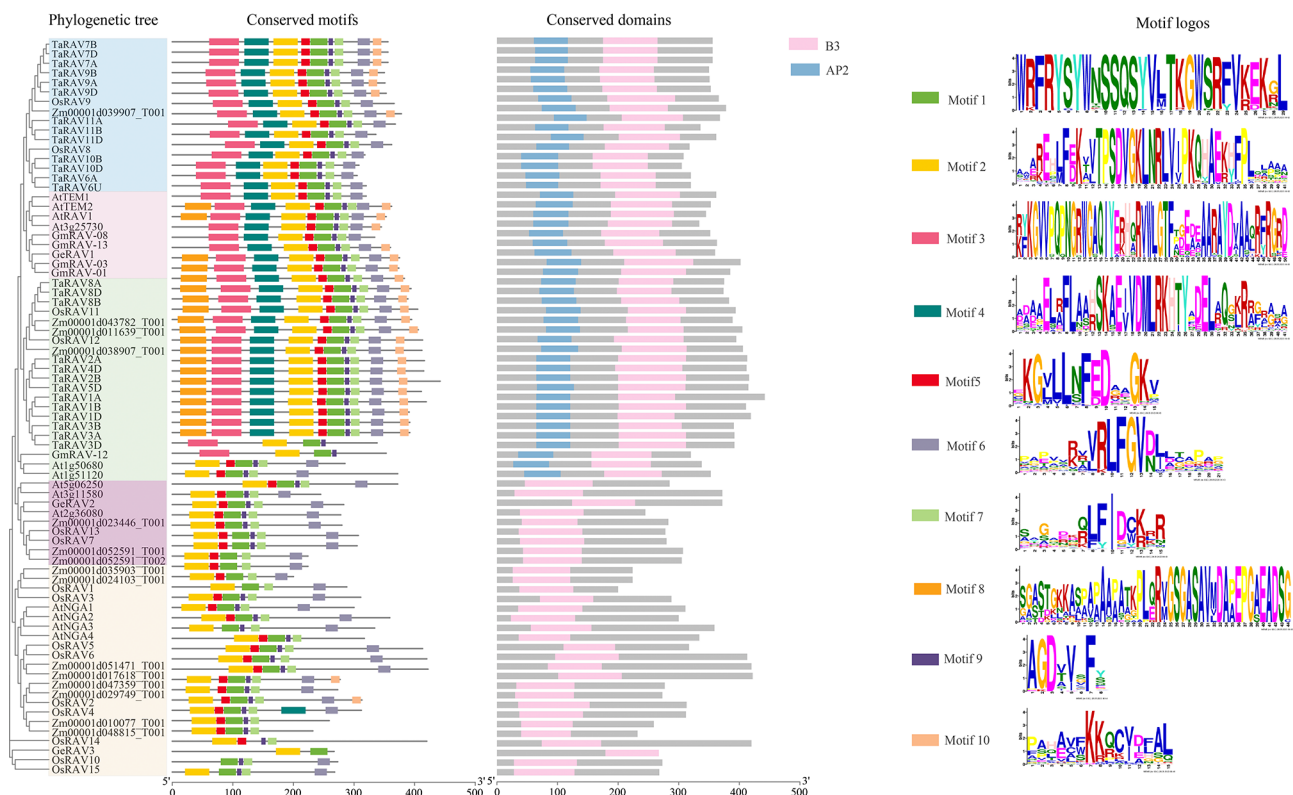


**Fig. 2** Phylogenetic tree, conserved motif, and conserved domain analyses of *GeRAV1* and other species RAVs. Phylogenetic tree: the phylogenetic tree was the same as the evolutionary tree in Fig. 1. Conserved motif: the 10 conserved motifs corresponded to ten boxes of different colors. Conserved domains: B3 domains and AP2 domains were shown as pink and blue boxes, respectively. Motif logos: ten motif logo patterns and sequences were shown in Table S6

that they were relatively conserved in *RAV* genes evolution. Besides, in terms of conserved domains, all *RAV* proteins have B3 domains at the C-terminus, but do not always contain both AP2 and B3 domains (Fig. 2). In addition, the proteins in the groups I, II, and III had both AP2 and B3 domains (Fig. 2).

#### The expression levels of *GeRAV* genes in response to low temperature stress

The expression profiles of the three *GeRAV* genes in *G. elegans* were analyzed under 4°C cold stress based on our transcriptomic data. The results showed that the expression of *GeRAV1* and *GeRAV2* were up-regulated under 4°C cold stress, whereas *GeRAV3* was down-regulated. *GeRAV1* exhibiting the highest expression profiles at 6 and 12 h (Fig. 3A). The qRT-PCR validation also showed that, under cold stress, the expression of *GeRAV1* gene maintained at a significant up-regulated level at 6, 12 and 24 h, which was about 4.75, 3.84 and 3.23 times higher than the control, respectively (Fig. 3B). Similarly, the expression of *GeRAV2* was also increased from 6 to 24 h, which was about 1.44, 1.77 and 1.67 times higher than the control, respectively (Fig. 3B). However, there was no significant change in the expression levels of the *GeRAV3*

gene (Fig. 3B). These findings indicated that the *GeRAV1* and *GeRAV2* genes were induced by cold stress with up-regulated expression.

#### Cloning and bioinformatics analysis of *GeRAV1*

As the *GeRAV1* gene was significantly up-regulated by low temperature stress (Fig. 3), its cDNA sequence (1272 bp) was amplified by RT-PCR using the RNA extracted from the leaves of *G. elegans* as a template. The *GeRAV1* gene contained an open reading frame (ORF) of 1083 bp, encoding a protein of 360 amino acids (Fig. S1) with a relative molecular weight of 40 kDa. The theoretical isoelectric point, the average hydrophilicity, and the instability coefficient of the *GeRAV1* protein was 9.12, -0.554, and 40.03, respectively, suggesting that it was an unstable and hydrophilic protein. The absence of a signaling peptide or transmembrane region in the *GeRAV1* protein indicated that it was a non-secretory protein. Secondary structure prediction results showed that the *GeRAV1* protein was mainly composed of a random coil (50.28%), alpha helix (23.89%), extended chain (19.72%), and beta-turn (6.11%) (Fig. S2).

Comparative analysis of the predicted tertiary structures revealed that the *GeRAV1* protein of *G. elegans*



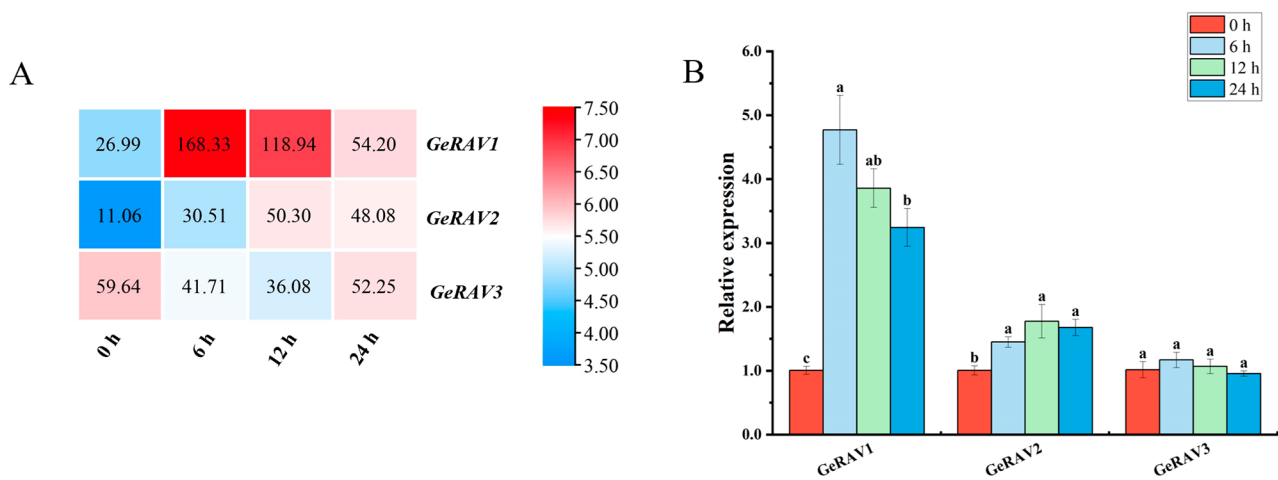


**Fig. 3** The expression of the *GeRAV* genes under 4°C low temperature treatment based on transcriptomic data (A) and qRT-PCR analysis (B). In Fig. A, the number of fragments per kilobase of transcript per million mapped reads (FPKM) in the boxes represented the expression levels of *GeRAVs*. The color bar represented the normalized values ( $\text{Log}_2$  FPKM). In Fig. B, *GeCUL* was used as the reference gene. Different lowercase letters on the bars indicated significant differences, determined by Duncan's new multiple range test ( $P < 0.05$ ). Data points represented mean  $\pm$  standard error ( $n = 3$ )

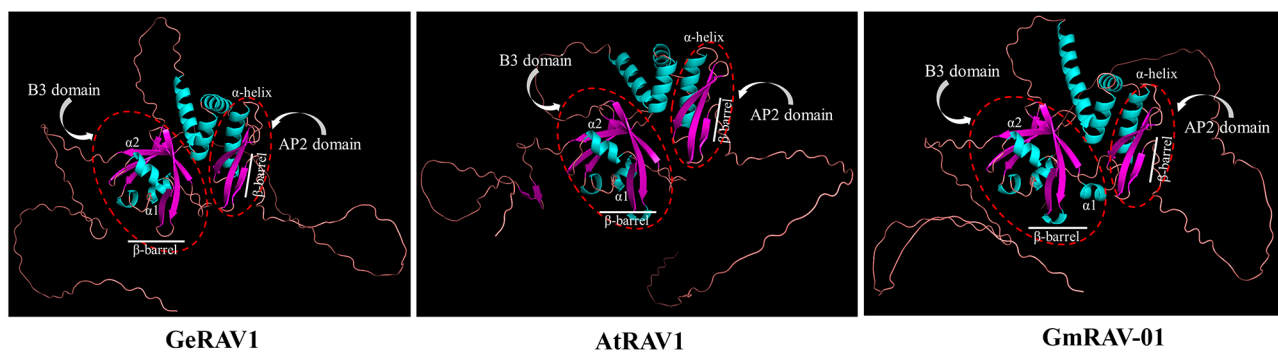


**Fig. 4** Predicted tertiary structures of *Gelsemium elegans* GeRAV1, *Arabidopsis thaliana* AtRAV1, and *Glycine max* GmRAV-01 proteins. The positions of the AP2 domain and the B3 domain were respectively outlined in red dotted lines. The AP2 domain included an  $\alpha$ -helix and a  $\beta$ -barrel protein, while the B3 domain included two  $\alpha$ -helices ( $\alpha 1$  and  $\alpha 2$ ) and a  $\beta$ -barrel protein

was highly similar to the RAV1 proteins of *A. thaliana* (At1g13260) and *G. max* (Glyma.01G22260). These three proteins contained an AP2 domain that consisted of an  $\alpha$ -helix and a  $\beta$ -barrel protein, and the  $\beta$ -barrel protein was located parallel to the  $\alpha$ -helix. In addition, the B3 domain of GeRAV1 contained two  $\alpha$ -helices and one  $\beta$ -barrel protein, where the  $\alpha$ -helices protruded from both ends of the  $\beta$ -barrel protein (Fig. 4). The amino acid sequence similarity of GeRAV1 with *Camptotheca acuminata* CaRAV (QNI23763.1), *Olea europaea* OeRAV1 (CAA2976529.1), *Vitis vinifera* VvRAV1 (XP\_002281709.2), *Carya illinoensis* CiRAV1-like (XP\_042963336.1), *G. max* GmRAV-03 (Glyma.02G11060), and *A. thaliana* AtRAV1 was 81.97%, 79.95%, 74.55%, 76.55%, 59.31%, and 60.50%, respectively (Fig. S3). Notably, their amino acid sequence of the AP2 and B3 domains were highly conserved. The amino acid sequence of GeRAV1 showed certain conservation, with

the N-terminal AP2 domain containing three  $\beta$ -strands (forming a  $\beta$ -barrel protein) and one  $\alpha$ -helix, and the C-terminal B3 domain containing seven  $\beta$ -strands (forming a  $\beta$ -barrel protein) and two  $\alpha$ -helices ( $\alpha 1$  and  $\alpha 2$ ) (Fig. S3). Furthermore, the predicted nuclear localization sequence (NLS) of the GeRAV1 protein was located at the C-terminus (Fig. S3).

#### Relative expression of *GeRAV1* gene in *G. elegans* tissues and under hormonal stress

Expression levels of *GeRAV1* in the tissues of *G. elegans* were determined using the qRT-PCR technique. The results showed that the *GeRAV1* gene was constitutively expressed in different tissues of *G. elegans*, with the highest expression levels in the roots, which was approximately 3.6 and 4.38 times higher than those in the leaves and stems, respectively (Fig. 5A). In addition, the expression of *GeRAV1* was induced by treatments with salicylic

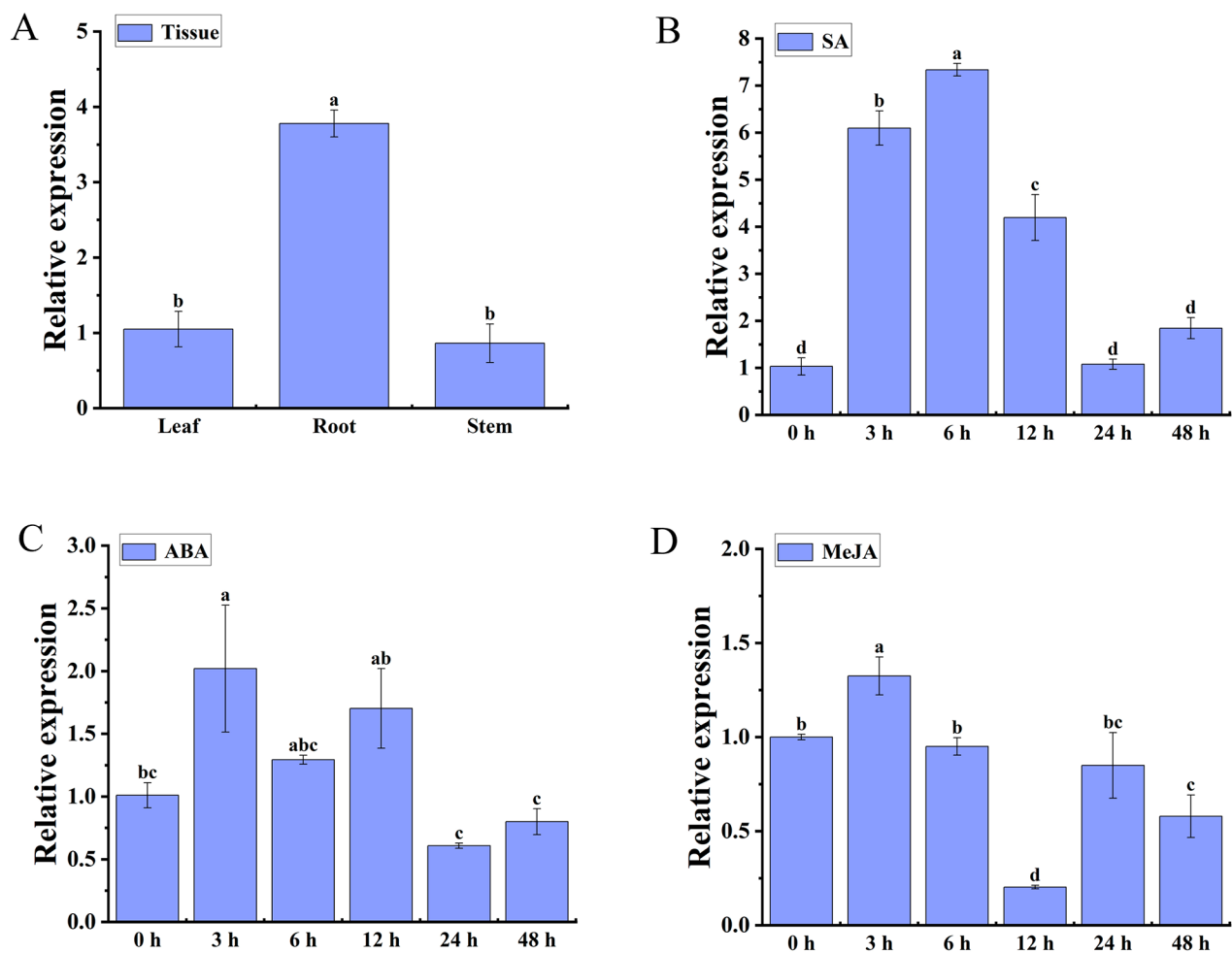


**Fig. 5** Relative expression analysis of the *GeRAV1* gene in different *Gelsemium elegans* tissues (A) and response to SA (B), ABA (C), and MeJA (D) stresses by qRT-PCR. *GeCUL* was used as the reference gene. Different lowercase letters on the bars indicated a significant difference, determined by Duncan's new multiple range test ( $P < 0.05$ ). Data points represented mean  $\pm$  standard error ( $n = 3$ )

acid (SA), abscisic acid (ABA), and methyl jasmonate (MeJA) (Fig. 5B, C, D). *GeRAV1* reached peak expression levels at 6 h under SA stress and at 3 h under both ABA and MeJA stimulus.

#### GeRAV1 was localized to the nucleus

Subcellular localization of the *GeRAV1* protein in the nucleus was predicted using WoLF PSORT and Plant-mPLOC online servers. To confirm this prediction, 35S::*GeRAV1*::GFP was used as an experimental group and 35S::GFP was used as a control group by *Agrobacterium*-mediated injections in *Nicotiana benthamiana* leaves. Confocal microscopy did not observe fluorescence signals in the control leaf cells, while the experimental group showed green fluorescence in the nucleus of leaf cells. Additionally, NbH2B (histone H2B) displayed red fluorescence in the nucleus of leaf cells. The overlap of green and red fluorescence resulted in yellow fluorescence, providing further evidence for the

subcellular localization of the *GeRAV1* protein in the nucleus (Fig. 6).

#### GeRAV1 had no self-activating activity

The presence of colonies on the tryptophan-deficient medium (SDO) plate of pGBKT7-*GeRAV1*, pGBKT7-p53+pGADT7-T (positive control), and pGBKT7 (negative control) indicated the successful transformation of recombinant plasmids into Y2HGold yeast (Fig. 7). The growth of colonies showed a consistent trend with the gradient of diluted liquid culture, indicating that the *GeRAV1* protein bound to GAL4-BD and expressed the missing tryptophan in the medium. Colonies of pGBKT7-*GeRAV1* were observed on the SDO/X- $\alpha$ -gal (5-bromo-4-chloro-3-indole- $\alpha$ -D-galactoside) (SDO/X) plate, as well as positive and negative controls. However, upon the addition of X- $\alpha$ -gal, only the positive control displayed blue color due to the activation of the *MEL1* reporter gene, while the rest of the samples showed no

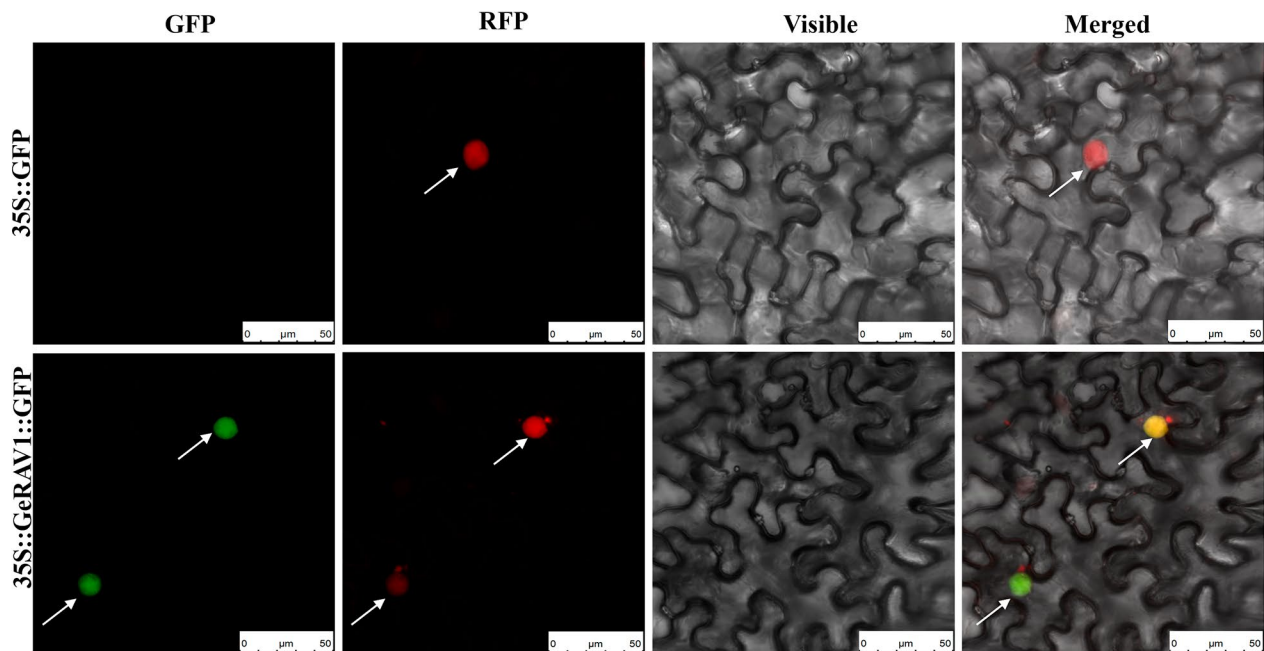


**Fig. 6** Subcellular localization of the GeRAV1 protein in *Nicotiana benthamiana*. The epidermal cells of *N. benthamiana* leaves were used for imaging analysis of bright field, green fluorescence (GFP), red fluorescence (RFP), and merged images of red and green fluorescence. White arrows indicated nucleus. Scale bar = 50  $\mu\text{m}$ . 35S::GFP: *Agrobacterium* strain carrying empty vector pFASTR05-GFP. 35S::GeRAV1::GFP: *Agrobacterium* strain carrying recombinant vector pFAST-R05-GeRAV1-GFP. pFAST-R05 expresses a gene fused to a GFP, which followed the *ccdB* gene (with a stop codon). NbH2B (histone H2B)-RFP was used to indicate the nucleus

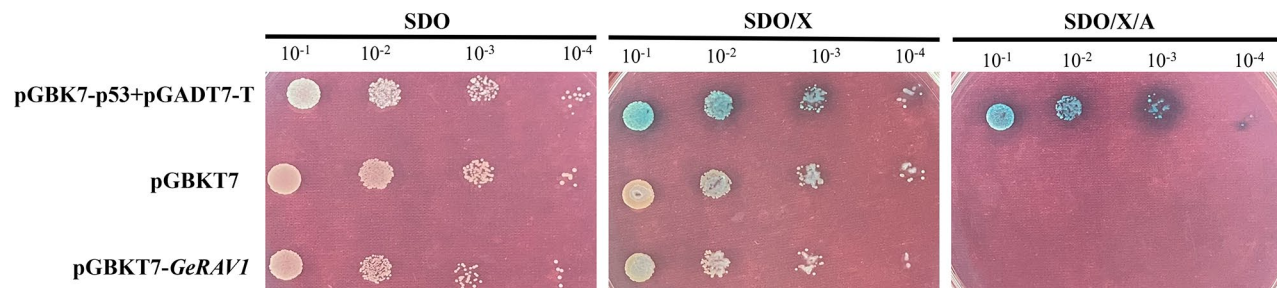


**Fig. 7** Transcriptional self-activation status of the GeRAV1 protein in yeast. SDO: Synthetic defined medium without tryptophan; SDO/X: synthetic defined medium without tryptophan supplemented with X- $\alpha$ -Gal; SDO/X/A: synthetic defined medium without tryptophan supplemented with X- $\alpha$ -Gal and aureobasidin A. pGBK7-p53+pGADT7-T: Positive control; pGBK7: negative control

color change, suggesting that the GeRAV1 protein had no self-activation activity. On the SDO/X/Aba (aureobasidin) (SDO/X/A) plate, only the positive control formed blue colonies, indicating activation of both *AURI-C* and *MEL1* reporter genes. In contrast, no colonies were observed for the negative control and pGBK7-GeRAV1 (Fig. 7), further confirming the absence of transcriptional self-activation activity in the GeRAV1 protein.

#### Stress tolerance assays of the GeRAV1 gene in *Escherichia coli* Rosetta (DE3)

The GeRAV1 protein has a predicted relative molecular weight of 40 kDa. pET32a expression vector contains

a 6 $\times$ His tag [36]. When recombinant cells (pET32a-GeRAV1-Rosetta) were successfully induced under specific conditions of 16 $^{\circ}\text{C}$ , 28 $^{\circ}\text{C}$ , 37 $^{\circ}\text{C}$ , and 0.7 mM isopropyl  $\beta$ -D-thiogalactoside (IPTG), an obviously accumulated protein was observed above 40 kDa (Fig. 8A). As shown in Fig. 8B, the recombinant cells (pET32a-GeRAV1-Rosetta) had similar growth conditions as the control cells (pET32a-Rosetta) with mannitol supplement. However, the growth of recombinant cells (pET32a-GeRAV1-Rosetta) was significantly better than that of the control cells (pET32a-Rosetta) when treated with low temperature treatment at 4 $^{\circ}\text{C}$  and sodium chloride (Fig. 8B). These results suggested that overexpression

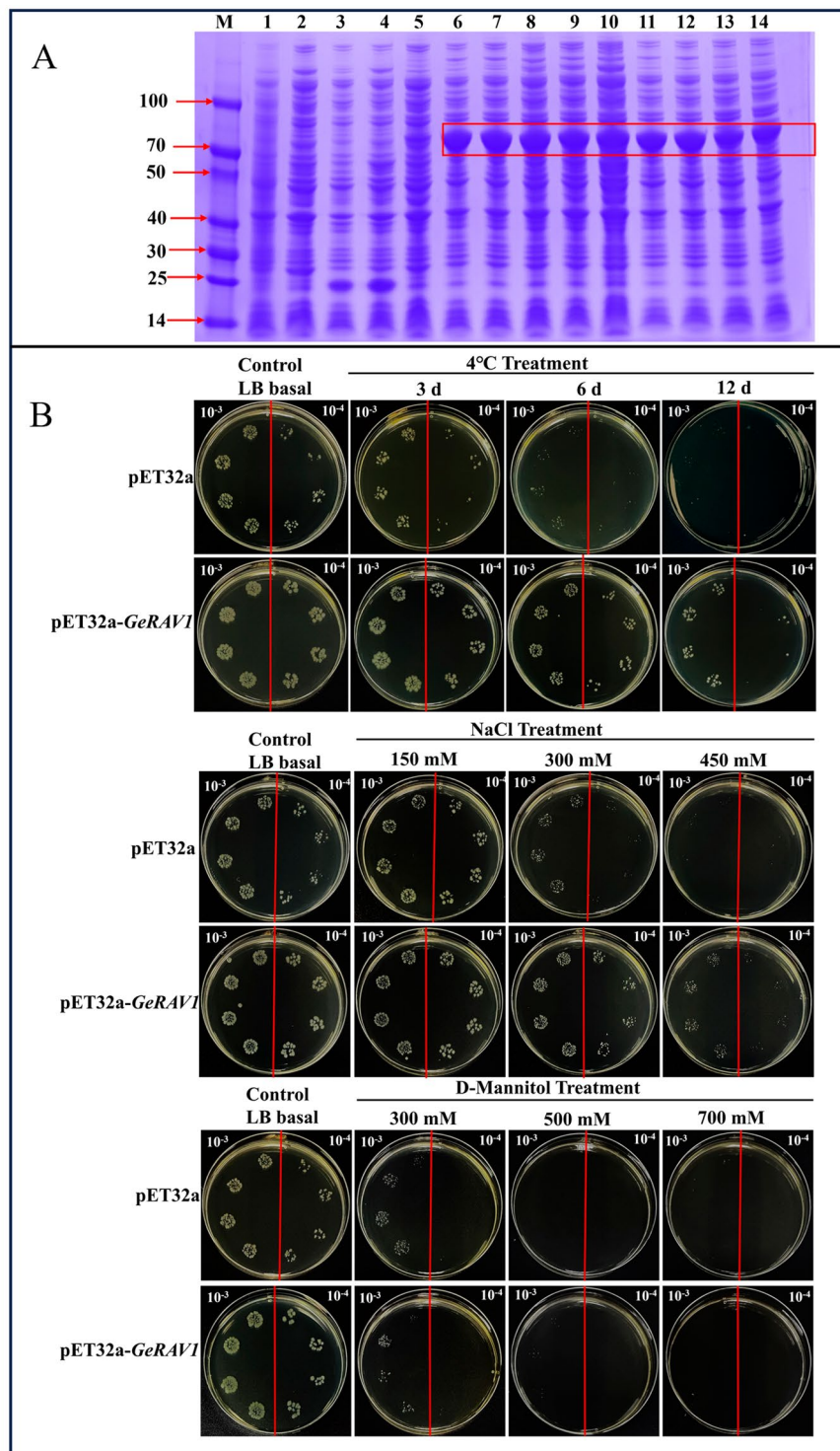


**Fig. 8** Expression analysis and plate stress validation of *GeRAV1* in *Escherichia coli* Rosetta (DE3) cells. **(A)** Induced expression of *GeRAV1* in *E. coli* Rosetta (DE3) cells. M: Protein marker; 1: blank control (uninduced *E. coli* Rosetta (DE3) cells); 2: blank control induced for 12 h; 3: control group (uninduced pET32a-Rosetta strain); 4: control group induced for 12 h; 5: uninduced recombinant strain (pET32a-*GeRAV1*-Rosetta strain); 6–10: recombinant strain induced at 37°C for 2, 4, 6, 8, and 12 h, respectively; 11–12: recombinant strain induced at 16°C for 2 and 12 h, respectively; 13–14: recombinant strain induced at 28°C for 2 and 12 h, respectively. The red boxes indicated the induced target protein. **(B)** Spot assay to verify the growth ability of pET32a-Rosetta cells and pET32a-*GeRAV1*-Rosetta cells on LB plates under 4°C, NaCl (sodium chloride), and mannitol stresses



of *GeRAV1* in *E. coli* Rosetta could enhance its tolerance to cold and NaCl stresses.

## Discussion

Plants have evolved a molecular regulatory network and cold resistance mechanisms to cope with low temperature stress. It has been found that plant cells sense changes in temperature upon low-temperature stimulation, which triggers signaling receptors, such as  $\text{Ca}^{2+}$  permeation channels, receptor kinases, histidine kinases. [1, 37]. Subsequently, led by substances such as  $\text{Ca}^{2+}$ , ABA, and reactive oxygen species, the low temperature signal was transmitted downward to activate TFs and regulate the expression of downstream CORs to enhance cold resistance [1, 37]. Within the AP2/ERF superfamily, the CBF/DREB TFs have been extensively and comprehensively studied in response to cold stress, as the CBF proteins can act on cis-acting elements and induce the expression of downstream CORs [1]. Recent research has identified RAV TFs belonging to the AP2/ERF family as cold-responsive TFs that may trigger regulatory pathways distinct from the CBF cold-responsive pathway [38]. Notably, RAV1 is a TF independent of the CBF pathway and plays a vital role in cold treatment and cold domestication [39]. Currently, RAV TFs respond positively to low temperature stress and have been cloned and studied in various plants such as *A. thaliana* [9], *O. sativa* [40], *Camellia sinensis* [41], *Galegae orientalis* [42], and *V. amurensis* [11].

## Sequences and phylogenetic characterization of *GeRAV1*

In this study, a *GeRAV1* gene with a significant response to low temperature stress was identified and characterized in the *G. elegans*. Tertiary structure prediction and multi-sequence alignments showed that the *GeRAV1* protein exhibited similar structural features to *AtRAV1* in *A. thaliana* (Fig. 4, Fig. S3), including the same number and the similar positions of  $\alpha$ -helices and  $\beta$ -sheets in the AP2 and B3 domains, that is, as well as other reported RAVs containing the AP2 and B3 domains [6, 33, 43]. In addition, the AP2 and B3 domains showed a high degree of conservation between different amino acid sequences of RAVs from various plant species (Fig. S3), suggesting their important role in DNA binding specificity [44]. Interestingly, we also found the highest homology of 81.97% between *G. elegans* *GeRAV1* and *C. acuminata* CaRAV (QNI23763.1) (Fig. S3). Therefore, it is hypothesized that there is a closer relationship between *G. elegans* and other genes in *C. acuminata*, which is conducive to our future research on alkaloid-related genes of *G. elegans*. Besides, *GeRAV1* clustered closely with *AtRAV1*, At3g25730, AtTEM1, AtTEM2, GmRAV-03, GmRAV-01, GmRAV-08, and GmRAV-13 (Fig. 1), indicating that there is a closer evolutionary relationship between

*GeRAV1* and two dicotyledonous plants (*A. thaliana* and *G. max*) than the other three monocotyledonous plants (*Z. mays*, *O. sativa*, and *T. aestivum*). *GmRAV-03* has been reported to enhance NaCl and drought tolerance in transgenic *A. thaliana*, but is insensitive to exogenous ABA [33]. *A. thaliana* *AtRAV1* has been found to be involved in the cold response [9]. *GeRAV1* belonged to the same group as GmRAV-03 and *AtRAV1*, with similar sequence type, number, and motif position (Fig. 2), indicating a similar biological function in the cold response. Previous studies have shown that the AP2 domain is a plant-specific domain involved in meristematic organization, flowering, seed development, and stress response [45]. The B3 domain binds to specific DNA and regulates plant growth, development, and hormone signaling [6, 46]. Considering that the *GeRAV1* protein contained both AP2 and B3 domains, it is possible that *GeRAV1* may not only play a regulatory role in cold stress but also affect the growth and development of *G. elegans* and participate in certain hormone signaling pathways.

## *GeRAV1* gene was constitutively expressed in various tissues and responded positively to cold stress

Differential expression of the *GhRAV* gene has been observed in roots, stems, and leaves of *Gossypium hirsutum*, with a more significant increase in expression in roots and stems [47]. We found that the *GeRAV1* gene in *G. elegans* was expressed in root, stem, and leaf tissues, with a higher expression level in roots (Fig. 5A). *G. elegans* roots have higher levels and types of alkaloids than leaves and stems [28, 48], which was consistent with previous findings that over half of the extracted monoterpene indole alkaloids come from roots [22]. In the present study, we confirmed that the *GeRAV1* gene was highly expressed in *G. elegans* roots, does this imply a potential role in regulating the synthesis and accumulation of alkaloids in the roots of *G. elegans*?

As reported, the *RAV* genes exhibited a response to cold stress [38]. In maize seedlings, the *ZmRAV3* gene was significantly overexpressed after treatment at 4°C for 2 h [49]. The expression of the *BraRAV-14* gene in *Chinese cabbage* was up-regulated under low temperature at 4°C, peaking at 24 h [50]. The *RAV* family genes in *Brassica napus* showed up-regulated expression at four time points (2, 6, 12, and 24 h), with nearly half of the *RAV* genes reaching their highest expression levels at 6 h [10]. Based on the transcriptome data and qRT-PCR analysis, three *GeRAV* genes were differentially expressed in *G. elegans* at 4°C (Fig. 3). Interestingly, the expression levels of the *GeRAV1* gene were significantly up-regulated from 6 to 24 h under 4°C treatment. In addition, prokaryotic expression analysis showed that *GeRAV1* enhanced the tolerance of *E. coli* cells to low temperature (4°C) and NaCl treatments (Fig. 8B). These results indicating the

potential role of the *GeRAV* gene in the response of *G. elegans* to low temperature and salt stresses. Similarly, previous studies have shown that *RAV* genes improved the tolerance of plants under NaCl and drought stresses [51, 52].

### Responses of *GeRAV1* to phytohormones stress

As one of the important signaling compounds, phytohormones can mediate plant response to abiotic stress [53]. The expression of the *GeRAV1* gene was significantly up-regulated at 3, 6 and 12 h under SA treatment and at 3 h under MeJA treatment (Fig. 5B, D), suggesting that the *GeRAV1* gene could be induced by SA and MeJA hormone stresses. Previous studies also showed that the expression of most *OsRAVs* in rice was up-regulated at 12 h under the treatments of MeJA and SA [35]. After challenging by ABA, the expression levels of *MtRAVs*, *GhRAV1*, and *GmRAV-03* were increased in *Medicago truncatula*, *Gossypium herbaceum*, and *G. max* [33, 54–56]. However, transgenic *A. thaliana* plants with the *MtRAVs*, *GhRAV1*, and *GmRAV-03* genes were insensitive to exogenous ABA, suggesting that these *RAV* genes might be participate in the ABA signaling pathway through an ABA-independent mechanism [33, 54–56]. In cucumber, *CsABI5* (ABA-associated marker gene) was significantly induced under ABA treatment and the transgenic *Arabidopsis* overexpressing *CsRAV1* was more tolerant to ABA, indicating that *CsRAV1* may directly regulate the expression of *CsABI5*, thereby participating in the ABA signaling pathway [57]. In this work, the *GeRAV1* gene was induced at 3, 6, and 12 h of ABA treatment (Fig. 5C). These results indicate that the *GeRAV1* gene of *G. elegans* may play a role in hormonal response. Further verification is needed to determine whether the *GeRAV1* gene is also involved in the ABA signaling pathway through an ABA-independent mechanism.

### Subcellular localization and transcriptional activation of *GeRAV1* protein

In plants, *RAV* TFs were involved in regulating biosynthesis and metabolism. Zhao et al. demonstrated that the *NnRAV1* gene could interact with the *NnbHLHI* gene to regulate the synthesis and accumulation of alkaloids in *Nelumbo nucifera* [58]. In *Solanum tuberosum*, the *StRAV1* gene regulated anthocyanin accumulation in tubers by repressing the expression of key anthocyanin biosynthesis structural genes such as *StCHS*, *StANS*, and *St3'5'H* by suppressing their promoters [59]. *McRAV1* acted as an inhibitor of anthocyanin biosynthesis in *Malus crabapple* [60]. Similarly, in *M. esculenta*, the CAACA motif in the *RAV* TFs was common in the promoters of melatonin biosynthesis-related genes. *MeRAV1* and *MeRAV2*, as upstream TFs, directly activated three melatonin biosynthesis genes in cassava [61].

The *FaRAV1* gene directly bound and activated the promoters in the anthocyanin biosynthetic pathway that promoted anthocyanin accumulation in *Fragaria ananassa* [62]. Previous research demonstrated that anthocyanins confer a variety of colors to organs such as flowers and fruits, and play important roles in resisting stressors like low temperature and bright light [63]. *RAV* TFs in various plant species have been reported to function as nucleoproteins, such as *G. max* GmRAV-01 [64], *G. orientalis* GoRAV [42], *Manihot esculenta* MeRAV1/2 [65], *M. truncatula* MtRAV1/2/3 [54], *A. thaliana* AtRAV1 [12], *Betula platyphylla* BpRAV1 [66], *Capsicum annuum* CaRAV1 [16], *G. herbaceum* GhRAV1 [56], and *Z. mays* ZmRAV1 [8]. Similarly, the subcellular localization results indicated that the *GeRAV1* was a nuclear-localized protein (Fig. 6). It is worth noting that ZmRAV1 in *Z. mays* and TaRAV1 in *T. aestivum* displayed transcriptional activity in yeast cells [8, 34], whereas NtRAV4 in *Nicotiana tabacum* did not [67]. In this study, the *GeRAV1* gene has no self-activation activity (Fig. 7), proving that it can be used as a bait, laying the foundation for mining functional genes that interact with it. This study will contribute to our further understanding of the biological function of the *G. elegans* *GeRAV1* gene. However, the role of *RAV* TFs in regulating biosynthesis and secondary metabolites in *G. elegans* still needs further investigation.

### Conclusion

In the present study, three novel *RAV* subfamily genes, whose encoding proteins were divided into three groups, were mined from the *G. elegans* transcriptome database under low temperature stress. Besides, the full-length *GeRAV1* gene, which was significantly induced by 4°C low temperature, was cloned and characterized. *GeRAV1* was a nucleoprotein without self-activating activity. The expression of *GeRAV1* was observed in all the *G. elegans* tissues and the transcripts mainly accumulated in roots. Furthermore, *GeRAV1* mRNA expression was up-regulated under SA, MeJA, and ABA stimulus. In particular, overexpression of *GeRAV1* could enhance the tolerance of *E. coli* Rosetta cells to low temperature and NaCl stresses, indicating that it is a potential candidate gene for genetic manipulation to improve low temperature and salt tolerance in *G. elegans*. These findings provide a basis for studying the biological functions and molecular regulatory mechanisms of *RAV* TFs in *G. elegans*.

### Materials and methods

#### *G. elegans* materials and treatments

The *G. elegans* plants were derived from Yongding District, Fujian Province, China (at an altitude of 602 m, coordinates: 116.9°E, 24.4°N). These plant materials were identified by Professor Zhongyi Zhang from Fujian

Agriculture and Forestry University as an evergreen woody vine plant belonging to the Loganiaceae family and Gelsemium genus. The roots, stems, and leaves of *G. elegans* were gathered and rapidly frozen in liquid nitrogen prior, and then stored in a -80°C freezer. Meanwhile, *G. elegans* seedlings were cultivated in a laboratory greenhouse under controlled conditions (25°C, 14 h of light, and 23°C, 10 h of darkness). Subsequently, the *G. elegans* plants with uniform growth were selected and subjected to the following four experiments. Under 4°C low temperature treatment, leaf samples were collected at 0, 6, 12, and 24 h [68]. The leaves of *G. elegans* were subjected to a foliar spray of 100 µM MeJA, 5 mM SA, and 100 µM ABA [69, 70], with leaf samples being collected at 0, 3, 6, 12, 24, and 48 h [70, 71].

#### Total RNA extraction and the first-strand cDNA synthesis

The *G. elegans* samples were ground to extract total RNA using the TRIzol method (Invitrogen, USA). According to the Hifair® cDNA Synthesis Kit (Yeasen, Shanghai, China), RNA from *G. elegans* leaves was reverse-transcribed into cDNA for subsequent gene cloning experiments. Based on the Hifair® cDNA Synthesis SuperMix kit (Yeasen, Shanghai, China), RNA of *G. elegans* tissues and *G. elegans* samples under different treatments was reverse-transcribed into cDNA and used as a template for qRT-PCR analysis.

#### Mining *GeRAV* genes from *G. elegans*

Based on the transcriptome database of *G. elegans* under 4°C treatment, three *GeRAV* genes, namely *GeRAV1* (c23896.graph\_c0), *GeRAV2* (c34018.graph\_c1), and *GeRAV3* (c35851.graph\_c0), were identified. The amino acid sequences of the RAV family members from *A. thaliana*, *O. sativa*, *Z. mays*, *G. max*, and *T. aestivum* were downloaded from TAIR, Phytozome, and Ensembl Plants databases [33–35] and were used for phylogenetic tree and conserved structural domains and motifs analyses with the three *GeRAV* proteins. Clustal X was used to perform multiple sequence comparisons. Evolutionary tree was constructed using MEGA X (Neighbor-Joining method, Bootstrap=1000) [72]. EvolView was employed to beautify the evolutionary tree [73]. For conserved motifs analysis, the number of motifs was set to 10 with other parameters remaining at their default values by MEME website [74]. The prediction of conserved domains was carried out using NCBI-CDD (Table S1). TBtools was used to visualize the outcomes of the evolutionary tree, conserved domains, and conserved motifs [75].

#### Cloning of *GeRAV1* gene and bioinformatics analysis

Based on the unigene sequence of the *GeRAV1* gene which has significant expression levels under low

temperature stress, its cloning primers (Table S2, Table S3) were designed using Primer 5.0. The PCR products were ligated into the Blunt-Zero vector (Yeasen, Shanghai, China). The *GeRAV1* ORF sequence was analyzed using the ORF-finder program. The physicochemical properties, signal peptides, and transmembrane regions of the *GeRAV1* protein were predicted using online software tools ProtParam, Net-Phos 3.1 server, SignalP 4.1 server, and TMHMM-2.0, respectively. The secondary structure of the protein was predicted using SOPMA. AlphaFold and PyMOL were used to predict and display the tertiary structure of the proteins, respectively [76]. Homologous amino acid sequences of *GeRAV1* were searched using NCBI-blastp online website. Sequence comparison of *GeRAV1* with other RAVs from the Dicot GenBank database was performed using DNAMAN6.0 software. The NLS was predicted using the online tool cNLS Mapper. The information of bioinformatics tools used was listed in Table S1.

#### Expression patterns of the *GeRAV* genes in different tissues and under various stresses

The expression levels of the *G. elegans GeRAV* genes under low-temperature, MeJA, ABA, and SA treatments were examined using qRT-PCR technology. The details of designing quantitative primers for the *GeRAV* genes were shown in Table S3. The *GeCUL* gene of *G. elegans*, previously screened by our research group, was used as the reference gene (not yet published). qRT-PCR reaction system followed the instructions of the ChamQ Universal SYBR qPCR Master Mix (Nazyne, Nanjing, China). The qRT-PCR reaction was performed using the QuantStudio™ 6 Flex real-time fluorescence quantitative PCR system. The melting and standard curves of the *GeRAV* genes were shown in Table S4. Each sample was performed in triplicate and sterile water was used as a control. Relative expression levels of the *GeRAV1* genes were calculated using the  $2^{-\Delta\Delta CT}$  method [77] and data significance analysis was conducted using SPSS 19.0.0. Origin 2022 was used for data visualization and plotting.

#### Subcellular localization

*GeRAV1* subcellular localization was predicted using WoLF PSORT and Plant-mPLOC server online tools (Table S1). Based on the gateway technology system, the primers Subloc-*GeRAV1*-F/R (Table S2) were designed. The positive plasmid pEASY-Blunt Zero-*GeRAV1* obtained by cloning was served as a template for the BP reaction [78]. The product was then ligated into the entry vector pDONR207 to produce the positive plasmid pDONR207-*GeRAV1*. Subsequently, an LR reaction (Invitrogen, USA) was performed to connect it to the subcellular localization vector pFAST-R05, which expresses a gene fused to the green fluorescent protein gene (*GFP*)

that follows the *ccdB* gene (with a stop codon) [79]. The positive recombinant plasmid pFAST-R05-*GeRAV1-GFP* (35S::*GeRAV1*::GFP) and the empty vector pFAST-R05-*GFP* (35S::GFP) were transformed into *A. tumefaciens* GV3101. After bacterial solution expansion and culture, the centrifuged culture was collected and washed twice with solution (10 mM magnesium chloride, 10 mM ethylmethylsulfone, pH=5.0-5.4), then resuspended and adjusted OD<sub>600</sub>≈0.6, followed by the addition of 200 μM acetosyringone. Post 2–3 h of induction under dark conditions, the solution was injected into *N. benthamiana* leaves of 5–6 leaf ages. A bacterial solution containing NbH2B (histone H2B) was also injected into the leaves of *N. benthamiana* [80]. Subcellular localization of the *GeRAV1* protein was observed using a Leica TCS SP8 confocal laser scanning microscope (Leica, Germany) after 2 days of incubation at 28°C and 16 h light/8 h dark.

### Transcriptional self-activation

The self-activation activity of *GeRAV1* was investigated using the Matchmaker Gold yeast two-hybrid system (with *AURI-C* and *MEL1* as reporter genes) [81]. First, the DNA-binding domain (BD) vector pGBKT7 was linearized by double digestion with *EcoRI* and *BamHI* restriction enzymes. Primers pGBKT7-*GeRAV1*-F/R (Table S2), designed with specific restriction sites, were used for PCR amplification and gel purification. Then, the linearized vector and gel-purified target fragment were ligated for homologous recombination using the ClonExpress II One Step Cloning Kit (Vazyme, Nanjing, China). Finally, the recombinant plasmid pGBKT7-*GeRAV1*, BD-pGBKT7 vector (negative control), and hybridization vector plasmid pGBKT7-53+pGADT7-T (positive control) were transformed into yeast Y2HGold competent cells (Weidi, Shanghai, China). After confirming the correctness of the cultures by PCR, the cultures were diluted to 1×10<sup>-1</sup>, 1×10<sup>-2</sup>, 1×10<sup>-3</sup>, and 1×10<sup>-4</sup>. Solid culture media including SDO, SDO/X, and SDO/X/A were prepared, and 7 μL of the diluted cultures were spotted onto the plates. All the plates were placed at 29°C for 2–3 d and photographed.

### Expression of *GeRAV1* gene in *E. coli* Rosetta (DE3) cells

According to the pET32a vector map, primers pET32a-*GeRAV1*-F/R (Table S2) were designed with restriction endonuclease sites *BamHI* and *HindIII* to obtain the recombinant plasmid pET32a-*GeRAV1*. Subsequently, the recombinant plasmid pET32a-*GeRAV1* and the pET32a vector were transformed into *E. coli* Rosetta (DE3) cells (TIANGEN, Beijing, China). The *E. coli* Rosetta (DE3) cells containing pET32a-*GeRAV1*, pET32a vector, and no vector were each cultured in 20 mL centrifuge tubes, respectively, and their OD<sub>600</sub> was adjusted between 0.6 and 0.7 and induced with 0.7 mM IPTG at

16°C, 28°C, and 37°C. All collected bacterial cultures were centrifuged and then loaded with a loading buffer. After boiling treatment at 100 °C, samples were subjected to sodium dodecyl sulfate-polyacrylamide gel electrophoresis for gel running. Following that, coomassie blue fast staining solution (Beyotime, Shanghai, China) was performed. The gel was then destained to observe the target bands. Finally, the FUSION FX.EDGE SPECTRA multi-color fluorescence & chemiluminescence (VILBER BIO IMAGING, Paris, France) was used for imaging.

The method of plate stress was used to investigate the response of *E. coli* Rosetta cells containing the *GeRAV1* gene under different stresses. When the bacterial cells (*E. coli* Rosetta (DE3) contains pET32a-*GeRAV1* and pET32a vectors, respectively) reached OD<sub>600</sub>=0.6, 0.7 mM IPTG was added to induce protein expression at 37°C. After 10 h of induction, the bacterial solution was adjusted to OD<sub>600</sub>=0.6 and then diluted again to 10<sup>-3</sup> and 10<sup>-4</sup>. A total of 10 μL dilution was spotted on the corresponding plate, and then the stress tests of low temperature at 4°C (3, 6, 12 d), sodium chloride (150, 300, and 450 mM) and mannitol (300, 500, and 700 mM) were performed. Afterward, they were placed in a 37°C incubator overnight for the growth of bacterial colonies and then photographed [82].

### Abbreviations

RAV	related to ABI3/VP1
ABA	abscisic acid
SA	salicylic acid
MeJA	methyl jasmonate
Tfs	Transcription factors
ICE-CBF/DREB	C-repeat binding factor expression/dehydration response elements binding protein
bZIP	leucine zipper
MYB	v-myb avian myeloblastosis viral oncogene homolog
NAC	NAM,ATAF1/2,CUC2
CORs	cold-regulated genes
AP2/ERF	APETALA2/ethylene-responsive factor
LTR	cis-acting elements involving low temperature response
FPKM	fragments per kilobase of transcript per million mapped reads
NLS	nuclear localization sequence
RT-PCR	reverse transcription PCR
qRT-PCR	real-time quantitative PCR
RNA-seq	RNA-sequencing
IPTG	isopropyl β-D-thiogalactoside
NaCl	sodium chloride
<i>E. coli</i> Rosetta	<i>Escherichia coli</i> Rosetta
SDO	tryptophan-deficient medium
X-α-Gal	5-bromo-4-chloro-3-indole-α-D-galactoside
AbA	aureobasidin
GFP	green fluorescent protein
RFP	red fluorescence protein

### Supplementary Information

The online version contains supplementary material available at <https://doi.org/10.1186/s12864-023-09919-9>.

Supplementary Material 1

Supplementary Material 2



### Acknowledgements

We are grateful to the reviewers for their helpful comments on the original manuscript. We would like to thank editors for their efficient works.

### Author contributions

T.C.: designed the experiments, formal analysis, and writing—original draft. S.Z., X.S., and J.Z.: performed the main experiments and data analysis. D.W., G.W. and R.C.: data analysis and paragraph review. Y.S., Y.Q., Q.L. and C.Y.: designed the experiments and writing—review and editing. C.Y. and Y.Q.: funding acquisition. All authors have read and agreed to the published version of the manuscript.

### Funding

This research was funded by Fujian Agriculture and Forestry University Science and Technology Innovation Special Fund Project (No. KFB23076) and Fujian Province College Student Innovation and Entrepreneurship Training Program Project (No. S202310389071).

### Data availability

The data supporting the conclusions of this article are within the paper.

### Declarations

#### Ethics approval and consent to participate

*G. elegans* (National Center for Biotechnology Information Taxonomy ID: 427660) is also known as Gou Wen in Chinese. We collected materials of *G. elegans* for this study. We processed the voucher specimens and stored them in the Fujian Key Laboratory of Sugarcane Biology and Genetic Breeding, Ministry of Agriculture and Rural Affairs, Fujian Agriculture and Forestry University (Fuzhou, China) with the accession numbers implad20230706. The work we reported here did not include any research on human participants or animals, nor did it involve any endangered or protected species. The experimental research on plants performed in this study complied with relevant institutional, national, and international guidelines and legislation. No specific permits are required for plant collection.

#### Consent for publication

Not applicable.

#### Competing interests

The authors have no conflict of interest to declare.

Received: 25 August 2023 / Accepted: 16 December 2023

Published online: 02 January 2024

### References

- Yang TW, Zhang LJ, Zhang TG, Zhang H, Xu SJ, An LZ. Transcriptional regulation network of cold-responsive genes in higher plants. *Plant Sci*. 2005;169:987–95.
- Ritonga FN, Ngatia JN, Wang Y, Khoso MA, Farooq U, Chen S. AP2/ERF, an important cold stress-related transcription factor family in plants: a review. *Physiol Mol Biol Pla*. 2021;27:1953–68.
- Mehrotra S, Verma S, Kumar S, Kumari S, Mishra BN. Transcriptional regulation and signalling of cold stress response in plants: an overview of current understanding. *Environ Exp Bot*. 2020;180:104243.
- Gu C, Gao ZH, Hao PP, Wang GM, Jin ZM, Zhang SL. Multiple regulatory roles of AP2/ERF transcription factor in angiosperm. *Bot Stud*. 2017;58:6.
- Kagaya Y, Ohmiya K, Hattori T. RAV1, a novel DNA-binding protein, binds to bipartite recognition sequence through two distinct DNA-binding domains uniquely found in higher plants. *Nucleic Acids Res*. 1999;27:470–8.
- Swaminathan K, Peterson K, Jack T. The plant B3 superfamily. *Trends in Plant Sci*. 2008;13:647–55.
- Kagaya Y, Hattori T. Arabidopsis transcription factors, RAV1 and RAV2, are regulated by touch-related stimuli in a dose-dependent and biphasic manner. *Genes Genet Syst*. 2009;84:95–9.
- Min HW, Zheng J, Wang JH. Maize *ZmRAV1* contributes to salt and osmotic stress tolerance in transgenic *Arabidopsis*. *J Plant Biol*. 2014;57:28–42.
- Fowler S, Thomashow MF. Arabidopsis transcriptome profiling indicates that multiple regulatory pathways are activated during cold acclimation in addition to the CBF cold response pathway. *Plant Cell*. 2002;14:1675–90.
- Du CF, Hu KN, Xian SS, Liu CQ, Fan JC, Tu JX, Fu TD. Dynamic transcriptome analysis reveals AP2/ERF transcription factors responsible for cold stress in rapeseed (*Brassica napus* L). *Mol Genet Genomics*. 2016;291:1053–67.
- Ren C, Li HY, Wang ZM, Dai Z, Lecourieux F, Kuang YF, Xin HP, Li SH, Liang C. Characterization of chromatin accessibility and gene expression upon cold stress reveals that the RAV1 transcription factor functions in cold response in *Vitis amurensis*. *Plant Cell Physiol*. 2021;62:1615–29.
- Woo HR, Kim JH, Kim J, Kim J, Lee U, Song IJ, Kim JH, Lee HY, Nam HG, Lim PO. The RAV1 transcription factor positively regulates leaf senescence in *Arabidopsis*. *J Exp Bot*. 2010;61:3947–57.
- Matías-Hernández L, Aguilar-Jaramillo AE, Marín-González E, Suárez-López P, Pelaz S. RAV genes: regulation of floral induction and beyond. *Ann Bot-London*. 2014;114:1459–70.
- Mandal D, Datta S, Ravindra G, Mondal PK, Chaudhuri RN. RAV1 mediates cytokinin signalling for regulating primary root growth in *Arabidopsis*. *Plant J*. 2023;113:106–26.
- Shin H, Nam KH. RAV1 negatively regulates seed development by directly repressing MIN13 and IKU2 in *Arabidopsis*. *Mol Cells*. 2018;41:1072.
- Sohn KH, Lee SC, Jung HW, Hong JK, Hwang BK. Expression and functional roles of the pepper pathogen-induced transcription factor RAV1 in bacterial disease resistance, and drought and salt stress tolerance. *Plant Mol Biol*. 2006;61:897–915.
- Wei X, Yang J, Ma HX, Ding CF, Yu H, Zhao YL, Liu YP, Khan A, Wang YF, Yang ZF, et al. Antimicrobial indole alkaloids with adductive C9 aromatic unit from *Gelsemium elegans*. *Tetrahedron Lett*. 2018;59:2066–70.
- Zhang W, Huang XJ, Zhang SY, Zhang D, Jiang RW, Hu JY, Zhang XQ, Wang L, Ye WC. Geleganindines A–C, unusual monoterpenoid indole alkaloids from *Gelsemium elegans*. *J Nat Prod*. 2015;78:2036–44.
- Zhang W, Xu W, Wang GY, Gong XY, Li NP, Wang L, Ye WC. Gelsekoumidines A and B: two pairs of atropisomeric bisindole alkaloids from the roots of *Gelsemium elegans*. *Org Lett*. 2017;19:5194–7.
- Li NP, Liu M, Huang XJ, Gong XY, Zhang W, Cheng MJ, Ye WC, Wang L. Gelsecorydines A–E, five gelsedine–corynanthe-type bisindole alkaloids from the fruits of *Gelsemium elegans*. *J Org Chem*. 2018;83:5707–14.
- Yamada Y, Kitajima M, Kogure N, Takayama H. Four novel gelsedine-type oxindole alkaloids from *Gelsemium elegans*. *Tetrahedron*. 2008;64:7690–4.
- Wang L, Chen SY, Gao X, Liang X, Lv WC, Zhang DF, Jin X. Recent progress in chemistry and bioactivity of monoterpenoid indole alkaloids from the genus *Gelsemium*: a comprehensive review. *J Enzym Inhib Med Ch*. 2023;38:2155639.
- Xu Y, Qiu HQ, Liu H, Liu M, Huang ZY, Yang J, Su YP, Yu CX. Effects of koumine, an alkaloid of *Gelsemium elegans* Benth., on inflammatory and neuropathic pain models and possible mechanism with allopregnanolone. *Pharmacol Biochem Be*. 2012;101:504–14.
- Cheng S, Chen C, Wang LL. Gelsemine exerts neuroprotective effects on neonatal mice with hypoxic-ischemic brain injury by suppressing inflammation and oxidative stress via Nrf2/HO-1 pathway. *Neurochem Res*. 2023;48:1305–19.
- Xu YK, Liao SG, Na Z, Hu HB, Li Y, Luo HR. Gelsemium alkaloids, immunosuppressive agents from *Gelsemium elegans*. *Fitoterapia*. 2012;83:1120–4.
- Liu M, Huang HH, Yang J, Su YP, Lin H, Lin LQ, Liao WJ, Yu CX. The active alkaloids of *Gelsemium elegans* Benth. are potent anxiolytics. *Psychopharmacology*. 2013;225:839–51.
- Liu D, Han Y, Zhou H, Jin HL, Kang H, Huang FF, Liu YF, Liang XM. Offline preparative three-dimensional HPLC for systematic and efficient purification of alkaloids from *Gelsemium elegans* Benth. *J Chromatogr A*. 2021;1640:461935.
- Wang J, Zhang J, Zhang CN, Sun XG, Liao X, Zheng W, Yin Q, Yang J, Mao DH, Wang B, et al. The qualitative and quantitative analyses of *Gelsemium elegans*. *J Pharmaceut Biomed*. 2019;172:329–38.
- Dong H, Li ML, Jin L, Xie XR, Li MF, Wei JH. Cool temperature enhances growth, ferulic acid and flavonoid biosynthesis while inhibiting polysaccharide biosynthesis in *Angelica sinensis*. *Molecules*. 2022;27:320.
- Palaniyandi K, Jun W. Low temperature enhanced the podophyllotoxin accumulation vis-a-vis its biosynthetic pathway gene(s) expression in *Diosma versipellis* (Hance) M. Cheng – a pharmaceutically important medicinal plant. *Process Biochem*. 2020;95:197–203.
- Yang DL, Sun P, Li MF. Chilling temperature stimulates growth, gene overexpression and podophyllotoxin biosynthesis in *Podophyllum hexandrum* Royle. *Plant Physiol Bioch*. 2016;107:197–203.

32. You CH, Liu AY, Zhang T, Zhao YF, Cui TZ, Xie JJ, Lin HL, Que YX, Su YC, Que WC. Identification of GeERF transcription factors in *Gelsmium elegans* and their expression under low temperature stress. *China J Chin Materia Med*. 2022;47:4908–18.
33. Zhao SP, Xu ZS, Zheng WJ, Zhao W, Wang YX, Yu TF, Chen M, Zhou YB, Min DH, Ma Y, et al. Genome-wide analysis of the RAV family in soybean and functional identification of *GmRAV-03* involvement in salt and drought stresses and exogenous ABA treatment. *Front Plant Sci*. 2017;8:905.
34. Luo YX, Chen SK, Wang PD, Peng D, Zhang X, Li HF, Feng CZ. Genome-wide analysis of the RAV gene family in wheat and functional identification of *TaRAV1* in salt stress. *Int J Mol Sci*. 2022;23:8834.
35. Chen CH, Li YJ, Zhang H, Ma Q, Wei Z, Chen J, Sun ZT. Genome-wide analysis of the RAV transcription factor genes in rice reveals their response patterns to hormones and virus infection. *Viruses*. 2021;13:752.
36. Su WH, Zhang C, Wang DJ, Ren YJ, Zhang J, Zang SJ, Zou WH, Su YC, You CH, Xu LP, et al. A comprehensive survey of the aldehyde dehydrogenase gene superfamily in *Saccharum* and the role of *ScALDH2B-1* in the stress response. *Environ Exp Bot*. 2022;194:104725.
37. Rihan HZ, Al-Issawi M, Fuller MP. Advances in physiological and molecular aspects of plant cold tolerance. *J Plant Interact*. 2017;12:143–57.
38. Yamasaki K, Kigawa T, Inoue M, Tatenno M, Yamasaki T, Yabuki T, Aoki M, Seki E, Matsuda T. Tomo et al. Solution structure of the B3 DNA binding domain of the Arabidopsis cold-responsive transcription factor RAV1. *Plant Cell*. 2004;16:3448–59.
39. Fowler SG, Cook D, Thomashow MF. Low temperature induction of *Arabidopsis* CBF1, 2, and 3 is gated by the circadian clock. *Plant Physiol*. 2005;137:961–8.
40. Yun KY, Park MR, Mohanty B, Herath V, Xu F, Mauleon R, Wijaya E, Bajic VB, Bruskiwicz R, de los Reyes BG. Transcriptional regulatory network triggered by oxidative signals configures the early response mechanisms of japonica rice to chilling stress. *BMC Plant Biol*. 2010;10:16.
41. Wu ZJ, Li XH, Liu ZW, Li H, Wang YX, Zhuang J. Transcriptome-based discovery of AP2/ERF transcription factors related to temperature stress in tea plant (*Camellia sinensis*). *Funct Integr Genomics*. 2015;15:741–52.
42. Chen XF, Wang Z, Wang XM, Dong J, Ren JZ, Gao HW. Isolation and characterization of *GoRAV*, a novel gene encoding a RAV-type protein in *Galegae orientalis*. *Genes Genet Syst*. 2009;84:101–9.
43. Nakano T, Suzuki K, Fujimura T, Shinshi H. Genome-wide analysis of the ERF gene family in *Arabidopsis* and rice. *Plant Physiol*. 2006;140:411–32.
44. Sakuma Y, Liu Q, Dubouzet JG, Abe H, Shinozaki K, Yamaguchi-Shinozaki K. DNA-binding specificity of the ERF/AP2 domain of *Arabidopsis* DREBs, transcription factors involved in dehydration- and cold-inducible gene expression. *Biochem Biophys Res Co*. 2002;290:998–1009.
45. Magnani E, Sjölander K, Hake S. From endonucleases to transcription factors: evolution of the AP2 DNA binding domain in plants. *Plant Cell*. 2004;16:2265–77.
46. Romanel EAC, Schrago CG, Couñago RM, Russo CAM, Alves-Ferreira M. Evolution of the B3 DNA binding superfamily: new insights into *REM* family gene diversification. *PLoS ONE*. 2009;4:e5791.
47. Kabir N, Lin H, Kong X, Liu L, Qanmber G, Wang YX, Zhang L, Sun ZJ, Yang ZR, Yu Y, et al. Identification, evolutionary analysis and functional diversification of RAV gene family in cotton (*G. hirsutum* L). *Planta*. 2022;255:14.
48. Lin HL, Qiu HQ, Cheng Y, Liu MB, Chen MH, Que YX, Que WC. *Gelsemium elegans* Benth: chemical components, pharmacological effects, and toxicity mechanisms. *Molecules*. 2021;26:7145.
49. Cheng C, An LK, Li FZ, Ahmad W, Aslam M, UI Haq MZ, Yan YX, Ahmad RM. Wide-range portrayal of AP2/ERF transcription factor family in maize (*Zea mays* L.) development and stress responses. *Genes-Basel*. 2023;14:194.
50. Li MY, Wang F, Jiang Q, Li R, Ma J, Xiong AS. Genome-wide analysis of the distribution of AP2/ERF transcription factors reveals duplication and elucidates their potential function in Chinese cabbage (*Brassica rapa* ssp. *pekinensis*). *Plant Mol Biol Rep*. 2013;31:1002–11.
51. Fu MJ, Kang HK, Son SH, Kim SK, Nam KH. A subset of *Arabidopsis* RAV transcription factors modulates drought and salt stress responses independent of ABA. *Plant Cell Physiol*. 2014;55:1892–904.
52. Wang SM, Guo T, Shen YX, Wang Z, Kang JM, Zhang JJ, Yi FY, Yang QC, Long RC. Overexpression of *MtRAV3* enhances osmotic and salt tolerance and inhibits growth of *Medicago truncatula*. *Plant Physiol Bioch*. 2021;163:154–65.
53. Waadt R, Seller CA, Hsu PK, Takahashi Y, Munemasa S, Schroeder JI. Plant hormone regulation of abiotic stress responses. *Nat Rev Mol Cell Biol*. 2022;23:680–94.
54. Wang SM, Guo T, Wang Z, Kang JM, Yang QC, Shen YX, Long RC. Expression of three related to ABI3/VP1 genes in *Medicago truncatula* caused increased stress resistance and branch increase in *Arabidopsis thaliana*. *Front Plant Sci*. 2020;11:611.
55. Finkelstein RR, Lynch TJ. The Arabidopsis abscisic acid response gene *ABI5* encodes a basic leucine zipper transcription factor. *Plant Cell*. 2000;12:599–609.
56. Li X, Li M, Zhou Y, Hu S, Hu R, Chen Y, Li XB. Overexpression of cotton *RAV1* gene in *Arabidopsis* confers transgenic plants high salinity and drought sensitivity. *PLoS ONE*. 2015;10:e0118056.
57. Li JL, Song CY, Li HM, Wang SQ, Hu L, Yin YL, Wang ZH, He WX. Comprehensive analysis of cucumber RAV family genes and functional characterization of *CsRAV1* in salt and ABA tolerance in cucumber. *Front Plant Sci*. 2023;14:1115874.
58. Zhao L. Mining and functional identification of alkaloid synthetic genes from lotus leaves. Fujian Agriculture and Forestry University; 2019.
59. Zhang HL, Zhao YN, Zhang ZH, Guo DL, Zhao X, Gao W, Zhang JP, Song BT. *StRAV1* negatively regulates anthocyanin accumulation in potato. *Sci Hortic-Amsterdam*. 2022;295:110817.
60. Li H, Han MZ, Yu LJ, Wang SF, Zhang J, Tian J, Yao YC. Transcriptome analysis identifies two ethylene response factors that regulate proanthocyanidin biosynthesis during *Malus crabapple* fruit development. *Front Plant Sci*. 2020;11:76.
61. Wei YX, Chang YL, Zeng HQ, Liu GY, He CZ, Shi HT. RAV transcription factors are essential for disease resistance against cassava bacterial blight via activation of melatonin biosynthesis genes. *J Pineal Res*. 2018;64:e12454.
62. Zhang ZY, Shi YN, Ma YC, Yang XF, Yin XR, Zhang YY, Xiao YW, Liu WL, Li YD, Li SJ, et al. The strawberry transcription factor FaRAV1 positively regulates anthocyanin accumulation by activation of *FaMYB10* and anthocyanin pathway genes. *Plant Biotechnol J*. 2020;18:2267–79.
63. Xie Y, Tan HJ, Ma ZX, Huang JR. DELLA proteins promote anthocyanin biosynthesis via sequestering MYB2 and JAZ suppressors of the MYB/bHLH/WD40 complex in *Arabidopsis thaliana*. *Mol Plant*. 2016;9:711–21.
64. Zhang KX, Zhao L, Yang X, Li MM, Sun JZ, Wang K, Li YH, Zheng YH, Yao YH, Li WB. *GmRAV1* regulates regeneration of roots and adventitious buds by the cytokinin signaling pathway in *Arabidopsis* and soybean. *Physiol Plant*. 2019;165:814–29.
65. Wang P, Yan Y, Bai YJ, Dong YB, Wei YX, Zeng HQ, Shi HT. Phosphorylation of *RAV1/2* by KIN10 is essential for transcriptional activation of *CAT6/7*, which underlies oxidative stress response in cassava. *Cell Rep*. 2021;37:110119.
66. Hu P, Zhang KM, Yang CP. Functional roles of the birch BpRAV1 transcription factor in salt and osmotic stress response. *Plant Sci*. 2022;315:111131.
67. Gao Y, Yang J, Duan WJ, Ma X, Qu LL, Xu ZC, Yang YX, Xu JY. *NtRAV4* negatively regulates drought tolerance in *Nicotiana tabacum* by enhancing antioxidant capacity and defence system. *Plant Cell Rep*. 2022;41:1775–88.
68. Tong N, Li D, Zhang ST, Tang MJ, Chen YK, Zhang ZH, Huang YJ, Lin YL, Cheng ZJ, Lai ZX. Genome-wide identification and expression analysis of the GRAS family under low-temperature stress in bananas. *Front Plant Sci*. 2023;14.
69. Soares AMS, Oliveira JTA, Gondim DMF, Domingues DP, Machado OLT, Jacinto T. Assessment of stress-related enzymes in response to either exogenous salicylic acid or methyl jasmonate in *Jatropha curcas* L. leaves, an attractive plant to produce biofuel. *S Afr J Bot*. 2016;105:163–8.
70. Zheng JR, Zhang X, Fu MY, Zeng H, Ye JB, Zhang WW, Liao YL, Xu F. Effects of different stress treatments on the total terpene trillactone content and expression levels of key genes in *Ginkgo biloba* leaves. *Plant Mol Biol Rep*. 2020;38:521–30.
71. Sun TT, Meng YT, Cen GL, Feng AY, Su WH, Chen YL, You CH, Que YX, Su YC. Genome-wide identification and expression analysis of the coronatine-insensitive 1 (*COI1*) gene family in response to biotic and abiotic stresses in *Saccharum*. *BMC Genomics*. 2022;23:38.
72. Kumar S, Stecher G, Li M, Knyaz C, Tamura K. MEGA X: molecular evolutionary genetics analysis across computing platforms. *Mol Biol Evol*. 2018;35:1547–9.
73. Subramanian B, Gao SH, Lercher MJ, Hu SN, Chen WH. Evolview v3: a web-server for visualization, annotation, and management of phylogenetic trees. *Nucleic Acids Res*. 2019;47:W270–5.
74. Bailey TL, Boden M, Buske FA, Frith M, Grant CE, Clementi L, Ren J, Li WW, Noble WS. MEME SUITE: tools for motif discovery and searching. *Nucleic Acids Res*. 2009;37:W202–8.
75. Chen CJ, Chen H, Zhang Y, Thomas HR, Frank MH, He YH, Xia R. TBtools: an integrative toolkit developed for interactive analyses of big biological data. *Mol Plant*. 2020;13:1194–202.

76. Mooers BHM. Shortcuts for faster image creation in PyMOL. *Protein Sci.* 2020;29:268–76.
77. Livak KJ, Schmittgen TD. Analysis of relative gene expression data using real-time quantitative PCR and the  $2^{-\Delta\Delta CT}$  method. *Methods.* 2001;25:402–8.
78. Su WH, Zhang C, Wang DJ, Ren YJ, Sun TT, Feng JF, Su YC, Xu LP, Shi MT, Que YX. The *CaCA* superfamily genes in *Saccharum*: comparative analysis and their functional implications in response to biotic and abiotic stress. *BMC Genomics.* 2021;22:549.
79. Wang DJ, Qin LQ, Wu MX, Zou WH, Zang SJ, Zhao ZN, Lin PX, Guo JL, Wang HB, Que YX. Identification and characterization of *WAK* gene family in *Saccharum* and the negative roles of *ScWAK1* under the pathogen stress. *Int J Biol Macromol.* 2023;224:1–19.
80. Yang S, Cai WW, Wu R, Huang Y, Lu QL, Wang H, Huang XY, Zhang YP, Wu Q, Cheng XG, et al. Differential CaKAN3-CaHSF8 associations underlie distinct immune and heat responses under high temperature and high humidity conditions. *Nat Commun.* 2023;14:4477.
81. Wang DJ, Wang L, Su WH, Ren YJ, You CH, Zhang C, Que YX, Su YC. A class III WRKY transcription factor in sugarcane was involved in biotic and abiotic stress responses. *Sci Rep.* 2020;10:20964.
82. Su WH, Ren YJ, Wang DJ, Su YC, Feng JF, Zhang C, Tang HC, Xu LP, Muhammad K, Que YX. The alcohol dehydrogenase gene family in sugarcane and its involvement in cold stress regulation. *BMC Genomics.* 2020;21:521.

### Publisher's Note

Springer Nature remains neutral with regard to jurisdictional claims in published maps and institutional affiliations.